Cell surface N-glycans influence electrophysiological properties and fate potential of neural stem cells

Andrew R. Yale[1,2,3]*, Jamison L. Nourse[2,3]*, Kayla R. Lee[2,3], Syed N. Ahmed[2,3], Janahan Arulmoli[3,4], Alan Y.L. Jiang[3,4], Lisa P. McDonnell[2,3], Giovanni A. Botten[5], Abraham P. Lee[4], Edwin S. Monuki [3,6], Michael Demetriou[2,7], and Lisa A. Flanagan[1,2,3,4]

[1] Department of Anatomy & Neurobiology

[2] Department of Neurology

[3] Sue & Bill Gross Stem Cell Research Center

[4] Department of Biomedical Engineering

[6] Department of Pathology and Laboratory Medicine

[7] Department of Microbiology and Molecular Genetics

University of California, Irvine, Irvine, CA, 92697, USA

[5] Department of Microbiology, Immunology & Molecular Genetics, University of California, Los Angeles, Los Angeles, CA, 90095, USA

*Equal contribution

Running title: N-glycans influence neural fate potential

Keywords: Neuron progenitor; astrocyte progenitor; glycosylation; biophysical; dielectrophoresis; membrane capacitance

Corresponding Author:

Lisa A. Flanagan, Ph.D.

Department of Neurology

University of California Irvine

3030 Gross Hall, 845 Health Sciences Road

Irvine, CA 92697-1705

tel: (949) 824-5786

email: lisa.flanagan@uci.edu

Summary:

Understanding the cellular properties controlling neural stem and progenitor cell (NSPC) fate choice will improve their therapeutic potential. The electrophysiological measure whole cell membrane capacitance reflects fate bias in the neural lineage but the cellular properties underlying membrane capacitance are poorly understood. We tested the hypothesis that cell surface carbohydrates contribute to NSPC membrane capacitance and fate. We found NSPCs differing in fate potential express distinct patterns of glycosylation enzymes. Screening several glycosylation pathways revealed that the one forming highly-branched N-glycans differs between neurogenic and astrogenic populations of cells *in vitro* and *in vivo*. Enhancing highly-branched N-glycans on NSPCs significantly increases membrane capacitance and leads to the generation of more astrocytes at the expense of neurons with no effect on cell size, viability, or proliferation. These data identify the N-glycan branching pathway as a significant regulator of membrane capacitance and fate choice in the neural lineage.

Introduction

Neural stem cells (NSCs) develop into neurons, astrocytes, and oligodendrocytes and understanding how choices are made among these different fates will improve the use of these cells in transplantation therapies (Cao et al., 2002). NSCs expanded *in vitro* for therapeutic purposes generate a heterogeneous population of neural stem and progenitor cells (NSPCs) with varying ratios of progenitors linked to distinct cell fates. The cell biological characteristics that distinguish cells biased toward forming neurons from those that will generate astrocytes are ill-defined and current cell surface markers limited. Understanding the intrinsic properties of neuron- and astrocyte-biased cells and the mechanisms that govern their fate will improve the ability to predict or control the differentiation potential of transplanted cells, enhancing the reproducibility and effectiveness of NSPC therapeutics.

A cell biological characteristic that predicts fate in many stem cell lineages is whole cell membrane capacitance, an electrophysiological property of the plasma membrane. Whole cell membrane capacitance can be used to identify and enrich cells at distinct stages of differentiation and is measured for living cells, non-invasively, without labels by dielectrophoresis (DEP) or impedance sensing. Analysis or sorting of NSPCs by DEP is not toxic since the short-term DEP exposure needed for these applications does not alter cell survival, proliferation, or differentiation (Lu et al., 2012). Membrane capacitance discriminates between undifferentiated cells and their differentiated progeny. NSPCs are distinguished from differentiated neurons and astrocytes and prospectively sorted from neurons by membrane capacitance using DEP (Flanagan et al., 2008; Prieto et al., 2012). Membrane capacitance defines and enables the enrichment of undifferentiated and differentiated cells in the hematopoietic stem cell (HSC), mesenchymal/adipose-derived stem cell (MSC/ADSC), and embryonic stem (ES) cell lineages, indicating the relevance of biophysical properties to fate across multiple stem cell types (for a recent review see (Lee et al., 2018)).

For NSCs and MSCs, inherent electrophysiological properties of undifferentiated cells predict their differentiated fate. The neurogenic and astrogenic fate potential of NSPC populations (both human and mouse) are reflected in distinct membrane capacitance values and membrane capacitance dynamically reflects declining neurogenic potential of human NSPCs (Labeed et al., 2011). Importantly, the sufficiency of membrane capacitance as a marker of fate in the neural lineage is shown by the enrichment of neurogenic or astrogenic cells from a mixed population of undifferentiated mouse NSPCs by DEP (Nourse et al., 2014; Simon et al., 2014). Similarly, the osteogenic fate potential of undifferentiated MSCs is detected by DEP (Hirota and Hakoda, 2011). Since the biophysical property whole cell membrane capacitance is linked to fate, determining the components contributing to this measure may reveal novel insights into processes governing cell differentiation.

The cellular and molecular structures influencing membrane capacitance are not well understood. The DEP frequencies used for stem cell analysis are not in the range used to detect resting membrane potential (Gheorghiu, 1993; Flanagan et al., 2008). Expression of a G protein-coupled receptor in yeast did not alter capacitance (Stoneman et al., 2007) although expression of channelrhodopsin-2 in HEK-293 cells did (Zimmermann et al., 2008), suggesting the possibility that certain membrane proteins can affect membrane capacitance. Based on biophysical theory, membrane capacitance should be impacted by plasma membrane surface area and thickness. While NSPCs that have distinct membrane capacitance values do not differ in size as measured by phase contrast microscopy (Labeed et al., 2011; Nourse et al., 2014), they may differ in membrane microdomains not visible at that level of resolution. Cell membrane microdomains such as ruffles or microvilli are expected to alter membrane capacitance by increasing cell surface area (Wang et al., 1994). Membrane thickness affected by the lipid composition of the plasma membrane has been proposed to influence whole cell membrane capacitance although there are constraints on the absolute thickness of the lipid bilayer set by the size of phospholipid head groups and fatty acid tails (Muratore et al., 2012). Modification of

vesicle phospholipid bilayers with polyethylene glycol (PEG) altered membrane capacitance (Desai et al., 2009), suggesting cell surface modifications could contribute to membrane capacitance of cells.

A cellular process that modifies the plasma membrane surface and impacts membrane microdomains is glycosylation, by which carbohydrates able to store charge are added to plasma membrane proteins and lipids. Domains of glycosylated cell surface molecules generate surface undulations to increase surface area (Zhao et al., 2002), create structures extending up to 200 nm from the cell surface so make "thickened" membrane structures (Paszek et al., 2014), and influence the protein makeup of the plasma membrane (Nabi et al., 2015). Glycosylation is critical for normal nervous system development (Haltiwanger and Lowe, 2004) and changes in glycosylation patterns during cortical brain development correlate with developmental periods of increased neuron or astrocyte production (Flaris et al., 1995; Ishii et al., 2007). Treatment of NSPCs with agents that modify cell surface carbohydrates alters their behavior in DEP (Nourse et al., 2014), leading to the hypothesis that glycosylation may impact membrane capacitance and fate of NSPCs.

Results

Neurogenic and astrogenic NSPCs exhibit differences in glycosylation enzymes

In the developing cerebral cortex, neurons are formed early (starting in mice at approximately embryonic day 10, E10) and neurogenesis decreases as astrocyte generation commences (around E16). Neurons and astrocytes are generated from NSPCs in the developing dorsal telencephalon stem cell niche (the ventricular zone/subventricular zone). In contrast, most cortical oligodendrocytes are generated ventrally in the ganglionic eminence and migrate into the cortex at later developmental stages (He et al., 2001). To test whether glycosylation patterns vary with fate potential, we isolated NSPCs from embryonic dorsal

forebrain at stages when either more neurons (E12) or astrocytes (E16) are formed (Qian et al., 2000). E12 neuron-biased and E16 astrocyte-biased cells differ in fate-specific membrane capacitance, making these cells reasonable tests for the contribution of glycosylation to this biophysical property (Labeed et al., 2011).

Glycosylation is controlled by enzymes in the endoplasmic reticulum (ER) and Golgi that sequentially add and remodel sugars (glycans) attached to proteins and lipids destined for expression on the cell surface or extracellular secretion. We compared RNA levels of glycosylation enzymes in E12 and E16 NSPCs and found multiple differentially expressed genes (Tables S1, S2, S3). Since membrane capacitance reflects characteristics of the plasma membrane, we prioritized enzymes expected to generate cell surface glycans so enzymes involved in ER quality control, targeting of enzymes to lysosomes, or lysosomal degradation of glycans were not considered further. We focused on N-glycosylation since virtually all cell surface proteins are N-glycosylated, and N-glycosylation controls function of membrane receptors mediating responses to extracellular cues. Loss of N-glycosylation enzymes causes defects in neural development (Schachter, 2001). N-glycosylation leads to formation of membrane microdomains affecting cell surface area, which is thought to impact capacitance. Most O-glycosylated proteins are secreted and many become components of the ECM, but some, such as the heparan sulfate proteoglycans glypican and syndecan can be membrane bound. Contributions of O-glycosylation to membrane capacitance and the combined effects of N- and O-glycosylation will be the focus of future studies.

N-glycosylation enzymes exhibiting a 1.2-fold or greater difference in expression between E12 and E16 NSPCs can be grouped by function (Fig. 1). N-acetylglucosaminyltransferases (such as MGAT3 and MGAT5) along with mannosidase II (MAN2A1 and MAN2A2) determine the degree of N-glycan branching. Sialyltransferases identified in the screen include ST6GAL1 that generates a terminal sialic acid and ST8SIA2 and

ST8SIA4 that work together to form polysialic acid. FUT8 and FUT11 are fucosyltransferases that add fucose residues to the core or terminal ends of N-glycans, respectively. B4GALT2 and B4GALT5 are galactosyltransferases that add galactose to N-glycans. B3GNT2 is an acetylglucosaminyltransferase that adds GlcNAc to N-glycans. The N-glycan branching, sialic acid, and fucose pathways were assessed further to test their association with fate in the neural lineage since multiple members of these pathways were identified in the screen and enzymes that perform different functions were associated with either E12 or E16 NSPCs.

Complex branching but not sialylation or fucosylation correlates with NSPC fate

N-glycan branching is controlled by enzymes that cleave excess mannose residues and initiate new N-glycan branches by attaching N-acetylglucosamine (GlcNAc)(Fig. 2A). High mannose N-glycans contain no GlcNAc branches while hybrid N-glycans contain both mannose and GlcNAc and complex N-glycans have lost all the excess mannose residues. RNA-seq analysis revealed high expression of N-glycan branching genes, including *Man1* isoforms, *Man2* isoforms, *Mgat1, Mgat2, Mgat3, Mgat4* isoforms, and *Mgat5* (Fig. 2B). NSPCs also express galectins, which bind N-glycans and modulate the activities of several N-glycan containing cell surface proteins. NSPCs express galectins 1, 4, 5, and 8 but little to no 2, 3, 7, 9, or 12 (Fig. 2B).

Gene expression analysis by qRT-PCR of *Mgat1*, the initial N-acetylglucosaminyltransferase in the pathway, and *Man2a1, Man2a2*, and *Mgat5* identified in the initial screen (Fig. 1) revealed significantly higher levels of *Mgat1* in E16 compared to E12 NSPCs (Fig. S1A). Matrix-assisted laser desorption/ionization time of flight (MALDI-TOF) mass spectrometry analysis suggested more N-glycans with 1 or 2 GlcNAc branches on E12 NSPCs but more with 3 or 4 on E16 cells (Fig. S1B). Lectin flow cytometry with fluorescein-conjugated leukocyte-phytohaemagglutinin (L-PHA), a plant lectin highly specific for MGAT5-generated highly-branched tetra-antennary N-glycans (Cummings and Kornfeld, 1982), detected higher but not significantly different L-PHA binding on E16 NSPCs compared to E12 cells (Fig. S1C).

We DEP sorted E12 NSPCs to generate a control and astrocyte-biased population (Nourse et al., 2014; Simon et al., 2014) from the same developmental stage since variation between E12 and E16 NSPCs could be due to their different ages independent of fate (Fig. 2C). We tested enrichment by analyzing undifferentiated cells for markers of astrocyte progenitors (Hartfuss et al., 2001; Sun et al., 2005; Chaboub et al., 2016) and differentiated cells for the formation of GFAP-positive astrocytes. As expected, the astrocyte progenitor markers *Asef* (*Arghgef4*), *Glast* (*Slc1a3*), and *Egfr* were more highly expressed in undifferentiated E16 NSPCs than in E12 cells (Fig. S1D). Expression of astrocyte progenitor markers in undifferentiated cells (Fig. 2D) and GFAP-positive astrocytes after differentiation (Fig. 2E) indicate that DEP sorting enriched astrocyte-biased cells. While some NSPCs express GFAP, control and sorted undifferentiated E12 NSPCs do not express GFAP (Fig. S1E) (Flanagan et al., 2008), confirming that this marker can be used to detect astrocyte differentiation from these cells. Analysis of both undifferentiated and differentiated cells indicate that sorting generated a more astrocyte biased population of cells (Fig. 2).

We used qRT-PCR to screen for differences in glycosylation enzyme expression between control and sorted astrocyte-biased NSPCs. Sorted cells express significantly higher levels of *Man2a1, Man2a2*, and *Mgat5* and a trend toward higher *Mgat1* compared to unsorted E12 NSPCs (Fig. 2F). Notably, sorted cells appear deficient in *Mgat3*, which prevents formation of highly-branched N-glycans (Brockhausen et al., 1988) and was higher in E12 NSPCs than E16 NSPCs in the initial screen (Figs. 1, 2F). Furthermore, highly-branched N-glycans detected by L-PHA were significantly elevated in sorted cells (MFI 19423 ± 2023) compared to unsorted control NSPCs (MFI 18101 ± 2092) (paired Student's t-test, $p=0.0157$). Together with the analysis of E12 and E16 NSPCs, the sorted cell data indicate a correlation between highly-branched N-glycans and fate of the cell population, suggesting this pathway may affect membrane capacitance and fate in the neural lineage.

The three enzymes that add sialic acid to N-glycans identified in the original screen of E12 and E16 NSPCs were *St6gal1*, which had higher expression in E16 NSPCs, and *St8sia2* and *St8sia4*, which were more highly expressed in E12 NSPCs (Fig. 1). Analysis by qRT-PCR indicated significantly higher levels of *St8sia2* and *St8sia4* in E12 NSPCs compared to E16 NSPCs but no difference in *St6gal1* (Fig S2A). MALDI-TOF studies suggested higher levels of sialic acid containing N-glycans on E12 compared to E16 NSPCs (Fig. S2B). Using the lectin *Sambucus nigra* agglutinin (SNA), we found no difference in terminal sialic acid residues generated by ST6GAL1 between E12 and E16 NSPCs (Fig. S2C). ST8SIA2 and ST8SIA4 form long polysialic acid (PSA) chains, most notably on the neural cell adhesion molecule (NCAM) to generate PSA-NCAM. PSA-NCAM was detected at lower levels on E16 NSPCs compared to E12 cells, but the difference was not significant (Fig. S2D). Neither *St8sia2* expression nor PSA-NCAM differed between the sorted astrocyte-biased population and unsorted NSPCs (Fig. S2E, F). Thus, while there may be more sialic acid on E12 than E16 NSPCs, potentially via the activities of ST8SIA2 and ST8SIA4 and not ST6GAL1, the lack of a difference in *St8sia2* and PSA expression in the sorted cells suggests this may not directly relate to fate. We previously found that isolation of PSA-NCAM positive cells from E12 NSPCs did not enrich for neuron-generating cells (Nourse et al., 2014). Furthermore, treatment of blood cells with neuraminidase to remove sialic acid did not change cell responses in DEP frequency ranges that probe the plasma membrane, indicating that the loss of sialic acid did not affect membrane capacitance (Burt et al., 1990). While E12 NSPCs have higher levels of PSA-generating enzymes than E16 NSPCs, there is not a clear link between PSA and fate-specific membrane capacitance.

Fucosylation of N-glycans occurs through the activities of fucosyltransferases (FUT). FUT8, which attaches a core fucose, showed the greatest difference in the original screen of E12 and E16 NSPCs and was higher in E16 cells (Fig. 1). Analysis of E12 and E16 NSPCs by qRT-PCR showed slightly higher but not significantly different levels of *Fut8* in the E16 sample (Fig S3A), and core-fucosylated N-glycans were slightly elevated in E16 NSPC membranes

compared to those from E12 as indicated by MALDI-TOF (Fig. S3B). However, lectin flow cytometry with *Lens culinaris* agglutinin (LCA), which detects core-fucosylated N-glycans, indicated similar levels of core fucose on E16 NSPCs and E12 NSPCs (Fig. S3C). Additionally, *Fut8* expression did not differ between the unsorted control NSPCs and the sorted astrocyte-biased population (Fig. S3D). Thus, the analysis of *Fut8* expression and activity in NSPCs did not provide evidence of a significant association between core fucosylation and fate in the neural lineage.

Highly-branched N-glycans increase in the brain stem cell niche as fate shifts from neurogenesis to astrogenesis

Development of the mammalian cerebral cortex proceeds in a stepwise pattern with neurons formed first (~E10 in mice) followed by astrocytes (~E16). The sequential generation of neurons and astrocytes provides a means to test association of glycosylation with fate *in vivo*. Cortical NSPCs reside in the ventricular zone/subventricular zone (VZ/SVZ) of the embryonic cerebral cortex, and differentiated cells migrate away from this region toward the pial surface to form the cortical plate (CP). We analyzed sagittal brain sections from E10-E18 embryos and used the NSPC markers Sry-box (SOX) 1 and SOX2 to mark the VZ/SVZ and microtubule associated protein 2 (MAP2) and doublecortin (DCX) as markers of differentiated neurons to define the CP (Fig. S4). Oligodendrocytes are not primarily generated in the cortex; most form ventrally in the ganglionic eminence and migrate to inhabit the cortex (dorsal telencephalon) at later embryonic stages, ~E18 (He et al., 2001). Thus, very few oligodendrocyte progenitors would be present in the cortical stem cell niche.

We used L-PHA lectin staining to assess highly-branched N-glycans in the VZ/SVZ stem cell niche and found significantly more L-PHA binding at E16 than at E12 (Fig. 3). There was no difference in staining of the CP at E12 and E16, showing that the differences in the VZ/SVZ were not due to general increases in highly-branched N-glycans in all regions of the cortex over

time. The levels of highly-branched N-glycans continue to increase in the VZ/SVZ NSPC niche at E18 as astrogenesis escalates (Figs. 3C, D, S5). Together with the results from cell culture studies, these data show that highly-branched N-glycans are associated with astrogenic NSPC populations both *in vitro* and *in vivo*.

GlcNAc treatment enhances expression of highly-branched N-glycans on E12 NSPCs and significantly increases membrane capacitance

We tested whether altering highly-branched N-glycans on the surface of E12 NSPCs changes their membrane capacitance values by supplementing the cells with N-acetylglucosamine (GlcNAc), which is readily taken up by cells and raises intracellular UDP-GlcNAc levels. The MGAT4 and MGAT5 branching enzymes are highly sensitive to availability of UDP-GlcNAc, and GlcNAc treatment increases N-glycan branching in a variety of cell types (Lau et al., 2007). GlcNAc treatment significantly increased highly-branched N-glycans detected by L-PHA on the surface of E12 NSPCs (Fig. 4). Increasing cell surface highly-branched N-glycans also caused a significant increase in whole cell membrane capacitance of E12 NSPCs, indicating a role for branched N-glycans in membrane capacitance (Fig. 4C).

Highly-branched N-glycans restrict neurogenesis without affecting NSPC size, viability, or proliferation

Highly-branched N-glycans may serve as markers of fate or may actively participate in fate decisions since glycosylation controls the function of myriad cell surface receptors, many with identified roles in fate decisions (Zhao et al., 2008). We assessed neuronal differentiation of control and GlcNAc treated E12 NSPCs to test whether highly-branched N-glycans impact fate. GlcNAc treatment led to a dose-dependent decrease in neuron formation, with significantly lower neurogenesis after treatment with 40 or 80 mM GlcNAc (Figs. 5A, B). There was no difference in cell size of control and 80 mM GlcNAc-treated NSPCs (Fig. 5C), consistent with

the fact that neither NSPCs that differ in fate (E12 and E16) nor astrocyte- and neuron-biased populations enriched from E12 NSPCs differ in size (Labeed et al., 2011; Nourse et al., 2014). GlcNAc supplementation might induce cell death, leading to the loss of cells biased to a particular fate. Yet there was no difference in cell viability or percentage of apoptotic cells between control and GlcNAc-treated NSPCs, suggesting cell death does not play a role in the effect of highly-branched N-glycans on fate (Fig. 5D). Highly-branched N-glycans could alter cell proliferation, impacting the percentage of neuron-biased cells in the population. However, two measures of cell proliferation (EdU incorporation and phosphorylated histone H3 expression) showed no differences between control and GlcNAc treated NSPCs (Fig. 5E). In sum, GlcNAc treatment to induce highly-branched N-glycans on E12 NSPCs decreases neurogenesis but not by altering cell size, viability, or proliferation.

Enhancing highly-branched N-glycans on undifferentiated NSPCs leads to the formation of more astrocytes at the expense of neurons

GlcNAc treatment effects could be due to branched N-glycans on undifferentiated NSPCs, on newly differentiated cells, or a combination of both since GlcNAc treatment spanned proliferation and differentiation stages (Fig. 5). Experiments were therefore designed to separate these effects by treating cells (1) when in the undifferentiated state (in proliferation medium), (2) as they differentiate (in differentiation medium), or (3) during both stages (throughout)(Fig. 6A).

GlcNAc treatment throughout both proliferation and differentiation stages led to a significant decrease in neuron formation (Fig. 6B, D, “throughout”) as seen in our initial experiments of neuron differentiation (Fig. 5). Treatment during only the proliferation stage induced a similar decrease in neuron formation, but treatment during the differentiation stage had no effect on the percentage of neurons (Fig. 6 B, D, “proliferation”, “differentiation”). These

data indicate that increasing cell surface highly-branched N-glycans decreases neurogenic potential of undifferentiated E12 NSPCs rather than affecting differentiated neurons.

Analysis of astrocyte generation from E12 NSPCs treated with GlcNAc revealed effects of highly-branched N-glycans on both undifferentiated and differentiated cells. Astrocyte quantitation was standardized by analyzing regions that did not contain dense clusters of cells and cell debris (Fig. S6) since astrocytes can become reactive in response to dying cells and upregulate GFAP expression, complicating analysis. GlcNAc treatment of undifferentiated NSPCs led to a significant increase in the percentage of astrocytes formed after differentiation (Fig. 6C, E, “proliferation”). Interestingly, treatment during the differentiation stage also significantly increased astrocyte percentages, suggesting effects of highly-branched N-glycans on the differentiated cells (Fig. 6C, E, “differentiation”). The percentage of astrocytes formed when GlcNAc treatment occurred throughout both proliferation and differentiation stages was significantly higher than that of cells treated just during proliferation, suggesting an additive effect on both undifferentiated and differentiated cells (Fig. 6C, E, “throughout”). Thus, highly-branched N-glycans impact the formation of astrocytes from NSPCs and also affect differentiated astrocytes.

At E12, cortical NSPCs primarily generate neurons and astrocytes and the number of cells in the cortex capable of making oligodendrocytes is low, in part since very few oligodendrocyte producing cells have migrated from the ganglionic eminence into the cortex at this stage (He et al., 2001). However, since E12 cortical NSPCs can generate low numbers of oligodendrocytes in culture (Qian et al., 2000), we assessed the effects of GlcNAc on oligodendrocyte generation. Oligodendrocyte percentages were significantly decreased when cells were treated with 80 mM GlcNAc during proliferation or throughout both proliferation and differentiation stages, but not when treated during differentiation only (Fig. S7). Since E12 NSPCs generate few oligodendrocytes, the biological significance of this finding is unclear and

further analysis should utilize cells isolated from the ganglionic eminence or other means to assess cells capable of generating higher numbers of oligodendrocytes.

GlcNAc is utilized in both N- and O-glycosylation, so we tested whether GlcNAc effects were specifically due to incorporation in N-glycan branching by pretreating cells with kifunensine (Kif). Kif is a highly specific inhibitor of mannosidase I and blocks the first steps of N-glycan branching (Fig. 2A) (Males et al., 2017). E12 NSPCs were pretreated with Kif and maintained in Kif during GlcNAc treatment to prevent GlcNAc incorporation into N-glycan branches (Fig. 7A). As indicated by L-PHA flow cytometry, Kif effectively blocked branching since no increase in branched N-glycans occurred with GlcNAc in the presence of Kif (Fig. 7B). No significant difference in neuron formation was observed between Kif treated NSPCs and cells treated with both Kif and GlcNAc, indicating Kif blocked the effect of GlcNAc on NSPC neurogenesis (Fig. 7C). Similarly, Kif prevented the effect of GlcNAc on astrogenesis since the Kif treated NSPCs did not differ from those treated with both Kif and GlcNAc (Fig. 7D). The ability of Kif to block the effects of GlcNAc indicates that GlcNAc influences the fate potential of NSPCs through the formation of branched N-glycans.

Discussion

We identify the N-glycosylation pathway leading to the formation of highly-branched N-glycans as a regulator of fate choice in the neural lineage and provide links between the expression of N-glycans on the cell surface and membrane capacitance, a novel label free biomarker of cell fate. Neurogenic and astrogenic NSPCs differ in expression of enzymes that lead to the formation of highly-branched N-glycans and these N-glycans increase in the stem cell niche *in vivo* as fate potential shifts from neurogenesis to astrogenesis. NSPCs induced to express more highly-branched N-glycans had significantly increased fate-specific membrane capacitance values, providing a direct link between cell surface glycosylation and this

biophysical property. Increasing the levels of NSPC highly-branched N-glycans specifically affected fate choice since GlcNAc treatment lead to the formation of greater percentages of astrocytes at the expense of neurons without affecting cell size, proliferation, or death. These data indicate that the N-glycan branching pathway is an important regulator of fate choice in the neural lineage.

Cell surface N-glycosylation significantly impacts membrane capacitance, a label-free measure of cell fate. Glycosylation likely affects capacitance values of many cell types since reductions in the complexity of the bacteria *C. difficile* S-layer, which is made up of glycoproteins and glycans on the bacterial envelope, induces shifts in membrane capacitance (Su et al., 2014). Glycosylation may contribute to membrane capacitance in other stem cell lineages; differentiation of MSCs to either adipogenic or osteogenic fates is associated with differences in both membrane capacitance (Bagnaninchi and Drummond, 2011) and glycosylation (Heiskanen et al., 2009; Hamouda et al., 2013). The interaction of membrane capacitance, cell fate, and cell surface glycosylation may have relevance for many cell types, including those in other stem cell lineages.

Cell surface glycosylation affects membrane structure and surface area, which are expected to impact whole cell membrane capacitance (Wang et al., 1994). The size of neuron- and astrocyte-biased NSPCs enriched by DEP did not differ (Nourse et al., 2014) and there was no difference in the size of untreated and GlcNAc-treated NSPCs in phase contrast microscopy although they differ in both membrane capacitance and fate (e.g. Figs. 4-6). Cell surface glycosylation affects formation of membrane microdomains such as microvilli and lipid rafts associated with membrane invaginations, and thus could lead to changes in surface area not visible by phase contrast (Zhao et al., 2002; Garner and Baum, 2008). The cell surface glycocalyx (glycoproteins, glycolipids, and galectins) can create thickened regions of membrane that may affect capacitance (Paszek et al., 2014). The shift in membrane capacitance of E12 NSPCs due to GlcNAc treatment (untreated: 8.2 +/- 0.2 mF/m^2; GlcNAc treated: 9.8 +/- 0.3

mF/m^2) (Fig. 4) is similar to the difference in membrane capacitance values of E12 and E16 NSPCs that differ in fate (E12: 8.2 +/- 0.5 mF/m^2; E16: 10.7 +/- 0.6 mF/m^2) (Labeed et al., 2011). Thus, cell surface highly-branched N-glycans could be sufficient to explain the fate-specific differences in capacitance of NSPCs.

Increasing highly-branched N-glycans on NSPCs alters fate potential, leading to the generation of more astrocytes and fewer neurons while not inducing changes in cell proliferation or viability. A direct role for branched N-glycans in NSPC differentiation has not been previously described, although glycosylation patterns shift in the cortex during developmental stages of increased neuron or astrocyte production (Ishii et al., 2007). Deletion of the N-glycan branching enzyme MGAT1 results in failed neural tube closure and embryonic lethality (Ioffe and Stanley, 1994). Loss of MGAT2 critical for the formation of branched N-glycans causes congenital disease with mental and psychomotor retardation (Schachter, 2001). The role of branched N-glycans in NSPC differentiation warrants further study.

The effects of highly-branched N-glycans on NSPCs could relate to N-glycan interactions with galectins. Galectin affinity is proportional to the number of sugar residues available for binding, so is increased when glycans are more branched and elongated from each branch point with N-acetyllactosamine (Lau et al., 2007; Nabi et al., 2015). Galectins may influence NSPC differentiation since NSPCs make galectin 1 (Fig. 2), which induces astrocyte maturation *in vitro* (Sasaki et al., 2004) and down-regulates neurogenesis in the adult rodent hippocampus (Imaizumi et al., 2011). Interaction of galectin 1 with the highly-branched N-glycans induced by GlcNAc may be part of the process leading to more astrocytes but fewer neurons from GlcNAc-treated E12 NSPCs.

N-linked glycosylation regulates multiple receptor classes and is thus well-poised to affect cell differentiation. N-glycan content governs plasma membrane receptor cell surface residence time and ligand affinity, affecting integrins that bind ECM (β1, α3, α5, αV), cell-cell adhesion proteins (cadherins), and receptors for growth factors and morphogens (e.g. EGFR,

PDGFR, gp130 subunit of CNTFR) (Pinho and Reis, 2015). The loss of MGAT5 and branching reduces cell responses to EGF, PDGF, bFGF, and IGF (Partridge et al., 2004). N-glycan branching governs cell proliferation through the regulation of growth-promoting (e.g. EGFR and PDGFR) and growth arrest receptors (e.g. TGFβR) that differ in numbers of N-glycan sites (Lau et al., 2007). Thus, differences in the cell surface glycosylation of neuron- and astrocyte-biased NSPCs may not only contribute to their distinct membrane capacitance values but also specifically regulate multiple types of receptors that guide fate.

Our data suggest MGAT5 may be more active in cells that will form astrocytes and MGAT3 in neuron-biased NSPCs, raising the possibility that the balance of these enzymes affects fate decisions. MGAT3 antagonizes the activity of MGAT5 since the formation of a bisecting N-glycan by MGAT3 prevents further branching by MGAT5 (Brockhausen et al., 1988). The *Mgat5* gene is more highly expressed in astrogenic-biased NSPCs (E16 and DEP-enriched) while the levels of *Mgat3* are higher in more neurogenic NSPC populations (E12 and unsorted) (Fig. 1, 2). GlcNAc treatment increases highly-branched N-glycans formed by MGAT5 leading to greater astrogenesis and reduced neurogenesis (Fig. 5, 6). Pluripotent stem cells that differentiate into neurons upregulate MGAT3 expression and have higher cell surface bisecting N-glycans, whereas differentiated astrocytes retain low levels of bisecting N-glycans (Terashima et al., 2014). The balance of MGAT3 and MGAT5 activity regulates several proteins impacting cell function. Overexpression of MGAT5 or loss of MGAT3 induces greater integrin-mediated migration, while high levels of MGAT3 cause reduced migration (Zhao et al., 2006). The generation of more bisecting N-glycans on cadherins fosters greater cell-cell adhesion whereas more highly-branched N-glycans decrease cell-cell adhesion (Guo et al., 2003; Pinho et al., 2009). The degree of MGAT3 and MGAT5-modified N-glycans on the cell surface of NSPCs could regulate responses to a variety of extracellular cues and thus alter fate potential.

Experimental Procedures

NSPC cell culture and GlcNAc treatment:

Mouse E12 or E16 NSPCs were isolated from the cerebral cortex, grown and differentiated as previously described (Lu et al., 2012). GlcNAc (Fisher Scientific) was prepared as a stock solution in media and supplemented in media daily. Full details for all experimental procedures are provided in Supplemental Experimental Procedures.

Immunocytochemistry and fate potential analysis:

NSPCs were fixed and stained with antibodies as previously described (Nourse et al., 2014). Cells double-positive for MAP2/DCX or MAP2/TUJ1 with neurites at least 3 times the length of the soma were counted as neurons. Cells expressing GFAP in a filamentous cytoskeletal pattern were counted as astrocytes.

RNA isolation, RNA sequencing and analysis:

RNA was isolated from E12 NSPCs, E16 NSPCs or E12 cerebral cortex as a control and cDNA synthesized using M-MLV reverse transcriptase. cDNA was analyzed using the RT^2 Profiler PCR Array (Qiagen) for 84 mouse glycosylation-related genes or qRT-PCR with primers for specific glycosylation enzymes.

Lectin flow cytometry:

Live NSPCs were labeled with lectins (e.g. 20 µg/mL FITC-conjugated L-PHA) (Vector Labs) and propidium iodide was used to exclude non-viable cells for analysis.

DEP-based NSPC sorting and capacitance measurements:

Mouse NSPCs were sorted using DEP devices and sorting parameters as previously described ensuring DEP had no effect on NSPC survival, proliferation or differentiation potential (Lu et al., 2012; Simon et al., 2014). Dissociated cells ($3x10^6$ cells/ml) were placed in DEP wells, electrodes were actuated at 100 kHz, 3 Vpp for 5 min or less, and cells attracted to the

electrodes were collected. Membrane capacitance measurements used the DEP-Well system (Labeed et al., 2011).

Brain tissue section analysis:

CD-1 mice brains were collected at E10, E12, E16, and E18 and sagittal sections (20 μm) stained with antibodies or lectins. Quantitative analysis used ImageJ to calculate signal intensity in at least 10 randomly selected areas within each layer (lectin-stained blood vessels were excluded). Minimum intensity values were subtracted from maximum values to control for variation in staining across samples.

Statistical Analysis:

Statistical analysis used Prism v6 software (GraphPad). Comparison of two samples utilized 2-tailed unpaired Student's t-tests except for qRT-PCR data obtained from E12 NSPCs and sorted cells, which was analyzed by a paired t-test since the same sample was measured before and after sorting. Data sets containing more than two samples were analyzed by one-way ANOVA. A Dunnett's *post hoc* correction was applied for the GlcNAc dose response experiments to compare all GlcNAc treatment groups to the untreated control and a Tukey's *post hoc* correction was applied for all other multiple comparisons.

Author contributions:

LAF, ARY, JLN conceived and designed the experiments. ARY, JLN, KRL, SNA, JA, AYLJ, LPM performed experiments. ARY, JLN, KRL, SNA, JA, GAB analyzed data. APL, ESM, MD provided expert advice. ARY, JLN, LAF wrote the manuscript. LAF supervised, supported the study, and finalized the manuscript.

Acknowledgements:

This work was supported in part by NSF CAREER Award IOS-1254060 (LAF), NIH NINDS T32 NS082174 (predoctoral fellowship to AY), CIRM RT1-01074 (LAF) and CIRM Bridges to Stem Cell Research at California State University, Fullerton TB-01181 (SNA), NIH NCRR and NCATS through Grant UL1 TR001414 (Pilot Grant to LAF), a Collaborative Multiple Sclerosis (MS) Research Center Award from the National MS Society (MD), the Sue & Bill Gross Stem Cell Research Center at University of California, Irvine, and a gift by Pearl Tze Hosfiel and Keith Hosfiel.

References

Bagnaninchi PO, Drummond N (2011) Real-time label-free monitoring of adipose-derived stem cell differentiation with electric cell-substrate impedance sensing. Proc Natl Acad Sci U S A *108*,6462-6467.

Brockhausen I, Narasimhan S, Schachter H (1988) The biosynthesis of highly branched N-glycans - studies on the sequential pathway and functional-role of N-acetylglucosaminyltransferases I, II, III, IV, V AND VI. Biochimie *70*,1521-1533.

Burt JP, Pethig R, Gascoyne PR, Becker FF (1990) Dielectrophoretic characterisation of Friend murine erythroleukaemic cells as a measure of induced differentiation. Biochim Biophys Acta *1034*,93-101.

Cao Q, Benton RL, Whittemore SR (2002) Stem cell repair of central nervous system injury. J Neurosci Res *68*,501-510.

Chaboub LS, Manalo JM, Lee HK, Glasgow SM, Chen F, Kawasaki Y, Akiyama T, Kuo CT, Creighton CJ, Mohila CA, Deneen B (2016) Temporal Profiling of Astrocyte Precursors Reveals Parallel Roles for Asef during Development and after Injury. J Neurosci *36*,11904-11917.

Cummings RD, Kornfeld S (1982) Characterization of the structural determinants required for the high affinity interaction of asparagine-linked oligosaccharides with immobilized Phaseolus vulgaris leukoagglutinating and erythroagglutinating lectins. J Biol Chem *257*,11230-11234.

Desai S, Vahey M, Voldman J (2009) Electrically Addressable Vesicles: Tools for Dielectrophoresis Metrology. Langmuir *25*,3867-3875.

Flanagan LA, Lu J, Wang L, Marchenko SA, Jeon NL, Lee AP, Monuki ES (2008) Unique dielectric properties distinguish stem cells and their differentiated progeny. Stem Cells *26*,656-665.

Flaris N, Shindler K, Kotzbauer P, Chand P, Ludwig C, Konstantinidou A, Roth K (1995) Developmentally-regulated lectin-binding in the embryonic mouse telencephalon. Brain Research *678*,99-109.

Garner OB, Baum LG (2008) Galectin-glycan lattices regulate cell-surface glycoprotein organization and signalling. Biochem Soc Trans *36*,1472-1477.

Gheorghiu E (1993) The resting potential in relation to the equivalent complex permittivity of a spherical cell-suspension. Physics in Medicine and Biology *38*,979-988.

Guo H, Lee I, Kamar M, Pierce M (2003) N-acetylglucosaminyltransferase V expression levels regulate cadherin-associated homotypic cell-cell adhesion and intracellular signaling pathways. Journal of Biological Chemistry *278*,52412-52424.

Haltiwanger RS, Lowe JB (2004) Role of glycosylation in development. Annu Rev Biochem *73*,491-537.

Hamouda H, Ullah M, Berger M, Sittinger M, Tauber R, Ringe J, Blanchard V (2013) N-Glycosylation Profile of Undifferentiated and Adipogenically Differentiated Human Bone Marrow Mesenchymal Stem Cells: Towards a Next Generation of Stem Cell Markers. Stem Cells and Development *22*,3100-3113.

Hartfuss E, Galli R, Heins N, Götz M (2001) Characterization of CNS precursor subtypes and radial glia. Dev Biol *229*,15-30.

He W, Ingraham C, Rising L, Goderie S, Temple S (2001) Multipotent stem cells from the mouse basal forebrain contribute GABAergic neurons and oligodendrocytes to the cerebral cortex during embryogenesis. Journal of Neuroscience *21*,8854-8862.

Heiskanen A, Hirvonen T, Salo H, Impola U, Olonen A, Laitinen A, Tiitinen S, Natunen S, Aitio O, Miller-Podraza H, Wuhrer M, Deelder A, Natunen J, Laine J, Lehenkari P, Saarinen J, Satomaa T, Valmu L (2009) Glycomics of bone marrow-derived mesenchymal stem cells can be used to evaluate their cellular differentiation stage. Glycoconjugate Journal *26*,367-384.

Hirota Y, Hakoda M (2011) Relationship between Dielectric Characteristic by DEP Levitation and Differentiation Activity for Stem Cells. Key Engineering Materials *459*,84-91.

Imaizumi Y, Sakaguchi M, Morishita T, Ito M, Poirier F, Sawamoto K, Okano H (2011) Galectin-1 is expressed in early-type neural progenitor cells and down-regulates neurogenesis in the adult hippocampus. Mol Brain *4*,7.

Ioffe E, Stanley P (1994) Mice lacking N-acetylglucosaminyltransferase I activity die at mid-gestation, revealing an essential role for complex or hybrid N-linked carbohydrates. Proc Natl Acad Sci U S A *91*,728-732.

Ishii A, Ikeda T, Hitoshi S, Fujimoto I, Torii T, Sakuma K, Nakakita S, Hase S, Ikenaka K (2007) Developmental changes in the expression of glycogenes and the content of N-glycans in the mouse cerebral cortex. Glycobiology *17*,261-276.

Labeed FH, Lu J, Mulhall HJ, Marchenko SA, Hoettges KF, Estrada LC, Lee AP, Hughes MP, Flanagan LA (2011) Biophysical characteristics reveal neural stem cell differentiation potential. PLoS One *6*,e25458.

Lau KS, Partridge EA, Grigorian A, Silvescu CI, Reinhold VN, Demetriou M, Dennis JW (2007) Complex N-glycan number and degree of branching cooperate to regulate cell proliferation and differentiation. Cell *129*,123-134.

Lee AP, Aghaamoo M, Adams TNG, Flanagan LA (2018) It's Electric: When Technology Gives a Boost to Stem Cell Science. Current Stem Cell Reports *4*,116-126.

Lu J, Barrios CA, Dickson AR, Nourse JL, Lee AP, Flanagan LA (2012) Advancing practical usage of microtechnology: a study of the functional consequences of dielectrophoresis on neural stem cells. Integr Biol *4*,1223-1236.

Males A, Raich L, Williams SJ, Rovira C, Davies GJ (2017) Conformational Analysis of the Mannosidase Inhibitor Kifunensine: A Quantum Mechanical and Structural Approach. Chembiochem *18*,1496-1501.

Muratore M, Srsen V, Waterfall M, Downes A, Pethig R (2012) Biomarker-free dielectrophoretic sorting of differentiating myoblast multipotent progenitor cells and their membrane analysis by Raman spectroscopy. Biomicrofluidics *6*,034113.

Nabi IR, Shankar J, Dennis JW (2015) The galectin lattice at a glance. J Cell Sci *128*,2213-2219.

Nourse JL, Prieto JL, Dickson AR, Lu J, Pathak MM, Tombola F, Demetriou M, Lee AP, Flanagan LA (2014) Membrane biophysics define neuron and astrocyte progenitors in the neural lineage. Stem Cells *32*,706-716.

Partridge EA, Le Roy C, Di Guglielmo GM, Pawling J, Cheung P, Granovsky M, Nabi IR, Wrana JL, Dennis JW (2004) Regulation of cytokine receptors by Golgi N-glycan processing and endocytosis. Science *306*,120-124.

Paszek MJ, DuFort CC, Rossier O, Bainer R, Mouw JK, Godula K, Hudak JE, Lakins JN, Wijekoon AC, Cassereau L, Rubashkin MG, Magbanua MJ, Thorn KS, Davidson MW, Rugo HS, Park JW, Hammer DA, Giannone G, Bertozzi CR, Weaver VM (2014) The cancer glycocalyx mechanically primes integrin-mediated growth and survival. Nature *511*,319-325.

Pinho S, Reis C, Paredes J, Magalhaes A, Ferreira A, Figueiredo J, Wen X, Carneiro F, Gartner F, Seruca R (2009) The role of N-acetylglucosaminyltransferase III and V in the post-transcriptional modifications of E-cadherin. Human Molecular Genetics *18*,2599-2608.

Pinho SS, Reis CA (2015) Glycosylation in cancer: mechanisms and clinical implications. Nature Reviews Cancer *15*,540-555.

Prieto JL, Lu J, Nourse JL, Flanagan LA, Lee AP (2012) Frequency discretization in dielectrophoretic assisted cell sorting arrays to isolate neural cells. Lab Chip *12*,2182-2189.

Qian X, Shen Q, Goderie SK, He W, Capela A, Davis AA, Temple S (2000) Timing of CNS cell generation: a programmed sequence of neuron and glial cell production from isolated murine cortical stem cells. Neuron *28*,69-80.

Sasaki T, Hirabayashi J, Manya H, Kasai K, Endo T (2004) Galectin-1 induces astrocyte differentiation, which leads to production of brain-derived neurotrophic factor. Glycobiology *14*,357-363.

Schachter H (2001) Congenital disorders involving defective N-glycosylation of proteins. Cellular and Molecular Life Sciences *58*,1085-1104.

Simon MG, Li Y, Arulmoli J, McDonnell LP, Akil A, Nourse JL, Lee AP, Flanagan LA (2014) Increasing label-free stem cell sorting capacity to reach transplantation-scale throughput. Biomicrofluidics *8*,064106.

Stoneman M, Chaturvedi A, Jansma D, Kosempa M, Zeng C, Raicu V (2007) Protein influence on the plasma membrane dielectric properties: In vivo study utilizing dielectric spectroscopy and fluorescence microscopy. Bioelectrochemistry *70*,542-550.

Su Y, Warren C, Guerrant R, Swami N (2014) Dielectrophoretic Monitoring and Interstrain Separation of Intact Clostridium difficile Based on Their S(Surface)-Layers. Analytical Chemistry *86*,10855-10863.

Sun Y, Goderie SK, Temple S (2005) Asymmetric distribution of EGFR receptor during mitosis generates diverse CNS progenitor cells. Neuron *45*,873-886.

Terashima M, Amano M, Onodera T, Nishimura S, Iwasaki N (2014) Quantitative glycomics monitoring of induced pluripotent- and embryonic stem cells during neuronal differentiation. Stem Cell Research *13*,454-464.

Wang X, Huang Y, Gascoyne P, Becker F, Holzel R, Pethig R (1994) Changes in friend murine erythroleukemia cell-membranes during induced-differentiation determined by electrorotation. Biochimica Et Biophysica Acta-Biomembranes *1193*,330-344.

Zhao FT, Li J, Shi GX, Liu Y, Zhu LP (2002) Modification of glycosylation reduces microvilli on rat liver epithelial cells. Cell Biol Int *26*,627-633.

Zhao YY, Takahashi M, Gu JG, Miyoshi E, Matsumoto A, Kitazume S, Taniguchi N (2008) Functional roles of N-glycans in cell signaling and cell adhesion in cancer. Cancer Sci *99*,1304-1310.

Zimmermann D, Zhou A, Kiesel M, Feldbauer K, Terpitz U, Haase W, Schneider-Hohendorf T, Bamberg E, Sukhorukov VL (2008) Effects on capacitance by overexpression of membrane proteins. Biochem Biophys Res Commun *369*,1022-1026.

Figure Legends

Figure 1. Differences in N-glycosylation enzyme gene expression between E12 and E16 mouse NSPCs. Thirty-two N-glycosylation enzyme genes were screened and 12 transcripts differed by more than 1.2-fold; 7 were higher in E16 astrocyte-biased (AB) NSPCs while 5 were higher in E12 neuron-biased (NB) NSPCs.

Figure 2. N-glycan branching correlates with NSPC fate. (A) Schematic representation of the N-glycans formed by glycosylation enzymes, culminating in the formation of highly-branched, complex N-glycans. (B) RNA-seq analysis of E12 NSPCs. Average RPKM (reads per kilobase of transcript per million mapped reads) values are organized from high (>1 RPKM) to low (<1 RPKM) expression. (C) In DEP sorting, E12 NSPCs are randomly distributed when the electric field is off. When the electric field is on, astrocyte-biased cells are attracted to electrode edges and neuron-biased cells are removed by flow, leaving an astrocyte biased population of sorted cells. (D) qRT-PCR analysis of astrocyte progenitor marker expression indicates sorted cells have significantly increased *Asef* (p=0.0239) and *Egfr* (p=0.0273) expression (paired Student's t-test). (E) Sorted cells generate more GFAP-positive cells after differentiation (p=0.0002, paired Student's t-test). (F) qRT-PCR analysis shows that sorted cells express higher levels of branching enzymes (*Man2a1*, p=0.0433, *Man2a2*, p=0.0474, *Mgat5*, p=0.0314; paired Student's t-test sorted vs. unsorted), while *Mgat3* that prevents branching appears decreased. All error bars represent standard error of the mean (SEM). N=3 or more independent biological repeats (*p<0.05, ***p<0.001).

Figure 3. N-glycan branching in the stem cell niche is high during astrogenic developmental stages *in vivo*. (A) L-PHA indicates highly-branched N-glycans in sagittal sections of the cerebral cortex at E12 and E16. Arrowheads point to blood vessels, which were excluded from analysis. Dotted boxes indicate example regions used for quantitative analysis (10 boxes or more were analyzed per layer in each section). More intense staining is evident in the E16 NSPC niche (VZ/SVZ) than the E12 niche (VZ). (B) Significantly greater staining in the

E16 NSPC niche but no difference in the CP (VZ/SVZ E12 vs. E16, p<0.0001; CP E12 vs. E16, p=0.1041, unpaired Student's t-test). (C) L-PHA staining increases in the NSPC niche (VZ/SVZ) from E10 to E18 without a corresponding increase in the CP. (D) Statistical analysis of the data in C indicates a significant increase in L-PHA intensity in the VZ/SVZ over time (p<0.0001, one-way ANOVA, Tukey *post hoc* for multiple comparisons). Error bars SEM. N=3 or more independent biological repeats, (**p<0.01, ***p<0.001, ****p<0.0001).

Figure 4. Enhancing N-glycan branching on the cell surface increases NSPC membrane capacitance. (A) Experimental design: suspended undifferentiated E12 NSPCs were grown in proliferation medium supplemented with 80 mM GlcNAc for 3 days then dissociated for analysis. (B) Flow cytometry with L-PHA indicates significantly more cell surface highly-branched N-glycans on GlcNAc treated cells compared to untreated (Untr) control cells (p=0.0219, unpaired Student's t-test). Error bars SEM. (C) Whole cell specific membrane capacitance (Cspec, mF= milliFarad) measured by DEP is significantly increased after GlcNAc treatment of E12 NSPCs (p=0.001, unpaired Student's t-test). Box plots depict 25th and 75th quartiles and median and the bars represent min and max values. N=3 or more independent biological repeats, (*p<0.05, ***p<0.001).

Figure 5. NSPCs with enhanced cell surface N-glycan branching form fewer neurons upon differentiation but do not differ in size, viability, or proliferation. (A) Neuron formation (MAP2) from E12 NSPCs treated with 0-80 mM GlcNAc for 3 days as undifferentiated cells and 3 days during differentiation. All nuclei labeled with Hoechst. (B) The percentage of MAP2/doublecortin (DCX) double-positive neurons formed from E12 NSPCs decreases with increasing GlcNAc concentration (one-way ANOVA, p<0.0001). *Post hoc* analysis by Dunnett's test: untreated E12 NSPCs vs. 40 mM (p=0.0002) and 80 mM (p<0.0001) GlcNAc treated cells. (C) Treatment with GlcNAc did not alter cell diameters of E12 NSPCs (p=0.3985, unpaired Student's t-test). (D) Cell viability live/dead assay denotes no effect of GlcNAc treatment on the

percentage of live E12 NSPCs (p=0.7569, unpaired Student's t-test). Annexin V flow cytometry indicated no difference in apoptosis acutely (~3-6 hours post treatment), 1 day, or 3 days after GlcNAc supplementation. Positive control cells were treated with 200 μM H_2O_2 for 3 hours to induce apoptosis. (E) NSPC proliferation measured by EdU incorporation (cells in S-phase) and phospho-histone H3 staining (cells in M-phase) was not affected by GlcNAc treatment (EdU p=0.7023, phospho-histone H3 p=0.4354, unpaired Student's t-tests). Error bars SEM. N=3 or more independent biological repeats, (***p<0.001, ****p<0.0001).

Figure 6. Increasing N-glycan branching on undifferentiated NSPCs decreases neurogenesis and increases astrogenesis upon differentiation. (A) Experimental design: E12 NSPCs were treated with 80 mM GlcNAc in proliferation media (undifferentiated cells, Proliferation, 3 days treatment), in differentiation media (as cells differentiate, Differentiation, 3 days treatment), or in both proliferation and differentiation (Throughout, 6 days treatment). Cells were in suspension during the proliferation stage then plated as adherent cells on laminin for differentiation. (B) Fewer neurons formed from GlcNAc-treated NSPCs during proliferation or throughout both stages compared to cells treated during differentiation or untreated controls. No obvious differences in neuronal morphology were noted in the different conditions. (C) More astrocytes were generated from GlcNAc-treated NSPCs than untreated controls (all treatment paradigms). (D) Significantly reduced MAP2/TUJ1 double-positive neurons from cells treated with GlcNAc during proliferation (Prolif) or throughout both stages (Through) compared to cells treated during differentiation (Diff) or untreated (Untr) control cells (Untr v Prolif p<0.0001, Untr v Through p<0.0001, Prolif v Diff p=0.0042, Through v Diff p=0.0002, one-way ANOVA, Tukey *post hoc* for multiple comparisons). These data indicate an effect of GlcNAc on undifferentiated NSPCs but not on differentiated neurons. (E) The percentage of GFAP-positive astrocytes was significantly increased in all GlcNAc-treated samples, showing effects of N-glycan branching on both undifferentiated NSPCs and differentiated cells (Untr v Prolif p=0.047, Untr v Through

p<0.0001, Untr v Diff p=0.0018, Prolif v Through p=0.0236, one-way ANOVA, Tukey *post hoc* for multiple comparisons). Error bars SEM. N=3 or more independent biological repeats, (*p<0.05, **p<0.01, ***p<0.001, ****p<0.0001).

Figure 7. Preventing GlcNAc from incorporating into the N-glycan branching pathway blocks GlcNAc effects on fate potential. (A) Experimental design: Undifferentiated E12 NSPCs were treated with either 0.5 μM Kif for 4 days, 80 mM GlcNAc for 3 days, or pre-treated with Kif 1 day prior to an additional 3 days of Kif + GlcNAc supplementation (Combo). Cells were differentiated for 3 days after treatment. (B) L-PHA flow cytometry analysis of cells after the 4 days of treatment indicates significantly lower highly-branched N-glycans on Kif and Combo treated cells compared to untreated controls (untreated v Kif or Combo p<0.0001, one-way ANOVA, Tukey *post hoc* for multiple comparisons). (C) No difference in neuronal differentiation between Kif and Combo treated cells, indicating no effect of GlcNAc in the presence of Kif. Combo treated cells show a slight decrease in neuron formation compared to untreated controls (untreated v Combo p=0.0311, one-way ANOVA, Tukey *post hoc* for multiple comparisons). (D) When blocked by Kif, GlcNAc has no effect on astrocyte formation since no difference was observed between Kif and Combo treated samples. Error bars SEM. N=3 or more independent biological repeats, (*p<0.05, ****p<0.0001).

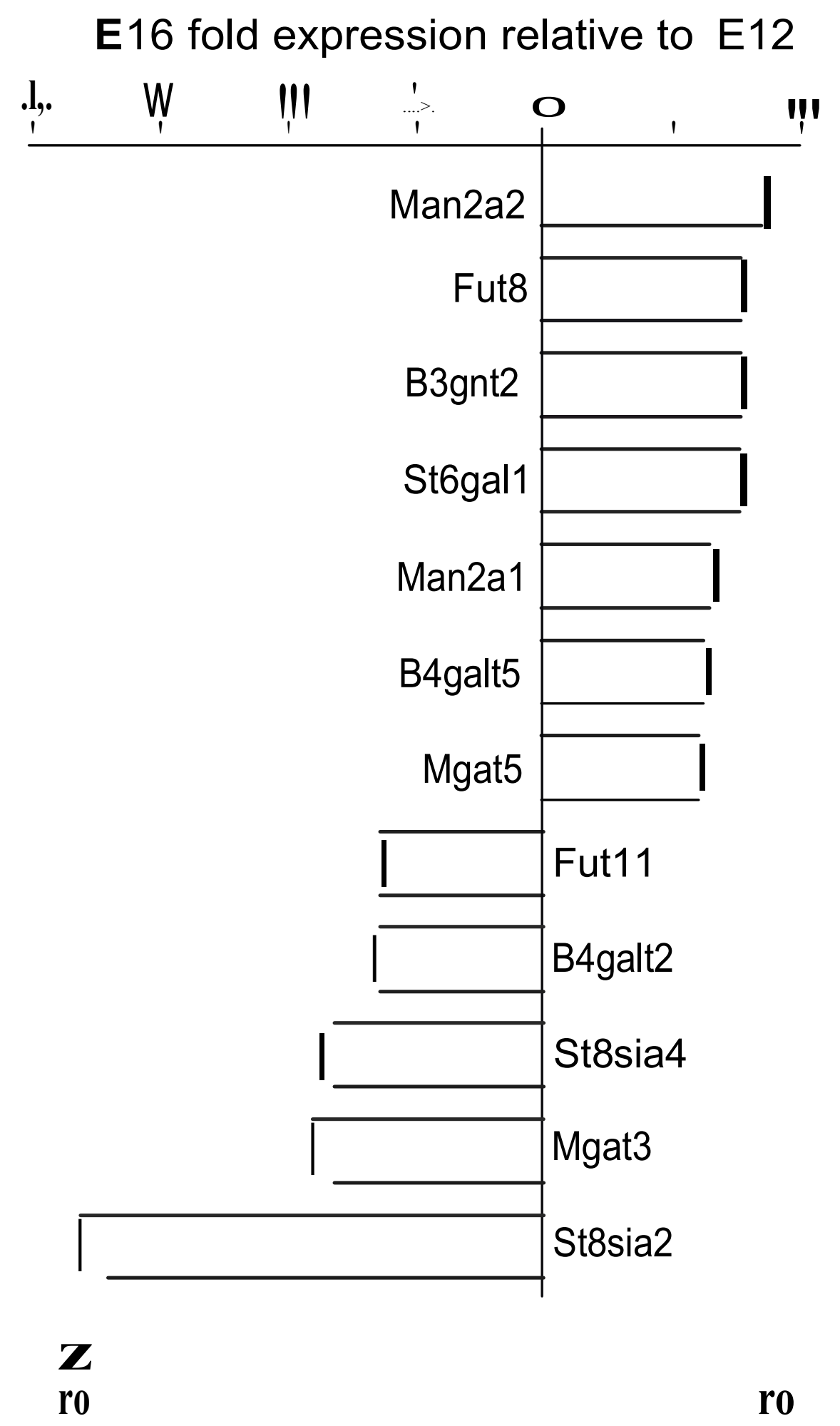
E16 fold expression relative to E12
Man2a2
Fut8
B3gnt2
St6gal1
Man2a1
B4galt5
Mgat5
Fut11
B4galt2
St8sia4
Mgat3
St8sia2

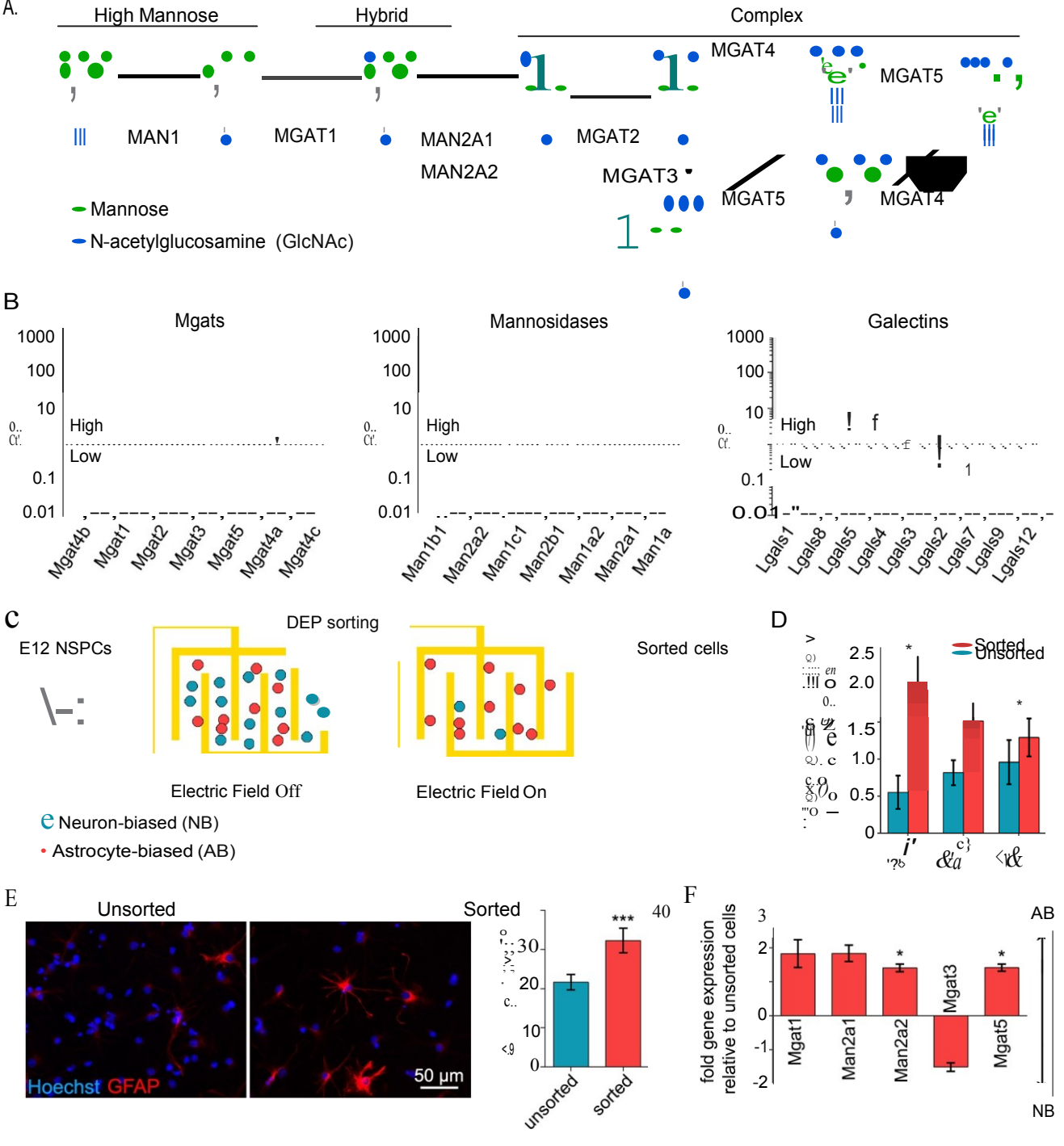
A.
High Mannose
Hybrid
Complex
MAN1
MGAT1
MAN2A1
MAN2A2
MGAT2
MGAT3
MGAT4
MGAT5
MGAT5
MGAT4
Mannose
N-acetylglucosamine (GlcNAc)
B
Mgats
Mannosidases
Galectins
High
Low
Mgat4b
Mgat1
Mgat2
Mgat3
Mgat5
Mgat4a
Mgat4c
Man1b1
Man2a2
Man1c1
Man2b1
Man1a2
Man2a1
Man1a
Lgals1
Lgals8
Lgals5
Lgals4
Lgals3
Lgals2
Lgals7
Lgals9
Lgals12
C
E12 NSPCs
DEP sorting
Sorted cells
Electric Field Off
Electric Field On
Neuron-biased (NB)
Astrocyte-biased (AB)
D
Sorted
Unsorted
E
Unsorted
Sorted
Hoechst GFAP
50 μm
unsorted
sorted
F
fold gene expression relative to unsorted cells
Mgat1
Man2a1
Man2a2
Mgat3
Mgat5
AB
NB

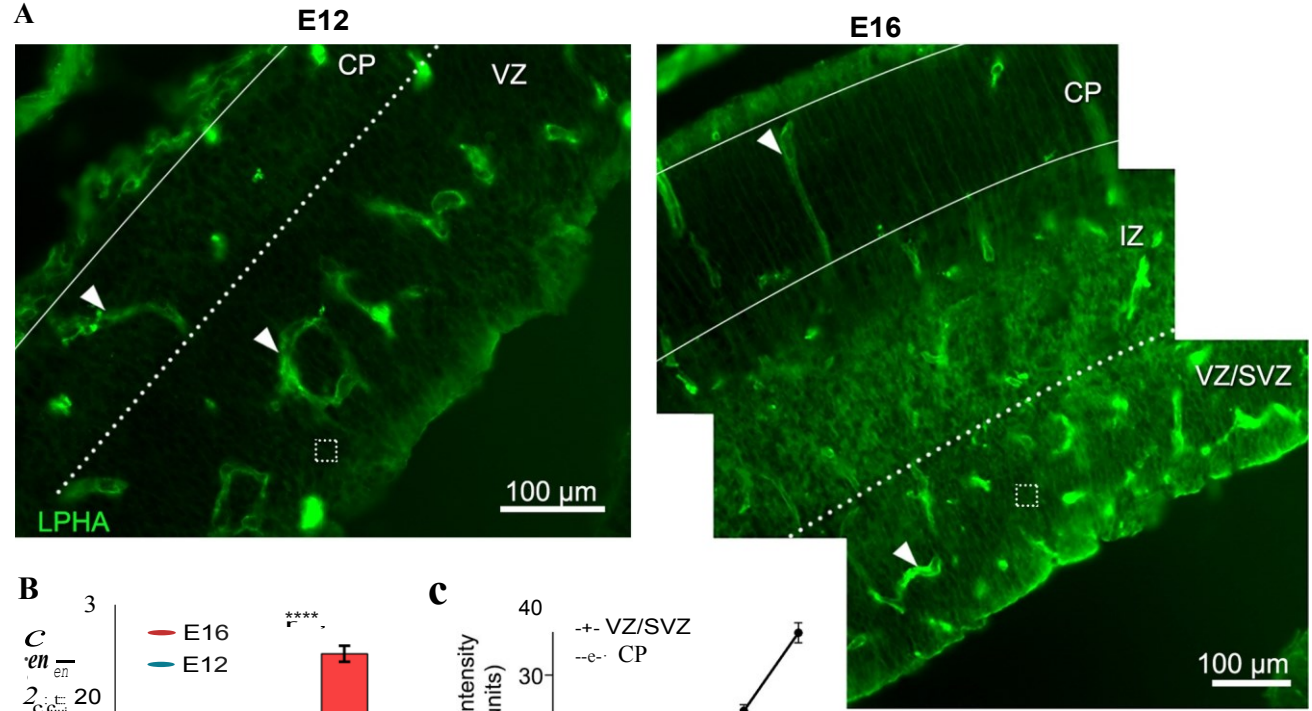

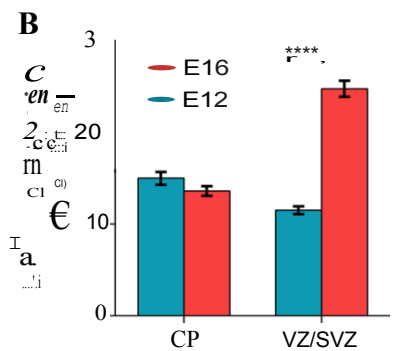

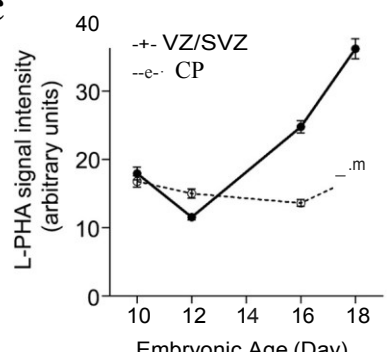

D

Cortical Plate

comparison	p-value	significance
E10 vs. E12	0.2628	ns
E10 vs. E16	0.0046	
E10 vs. E18	0.9208	ns
E12 vs. E16	0.4619	ns
E12 vs. E18	0.0735	ns
E16 vs. E18	0.0005	

Ventricular/Sub-ventricular Zone

comparison	p-value	significance
E10 vs. E12	0.0001	
E10 vs. E16	<0.0001	
E10 vs. E18	<0.0001	
E12 vs. E16	<0.0001	
E12 vs. E18	<0.0001	
E16 vs. E18	<0.0001	

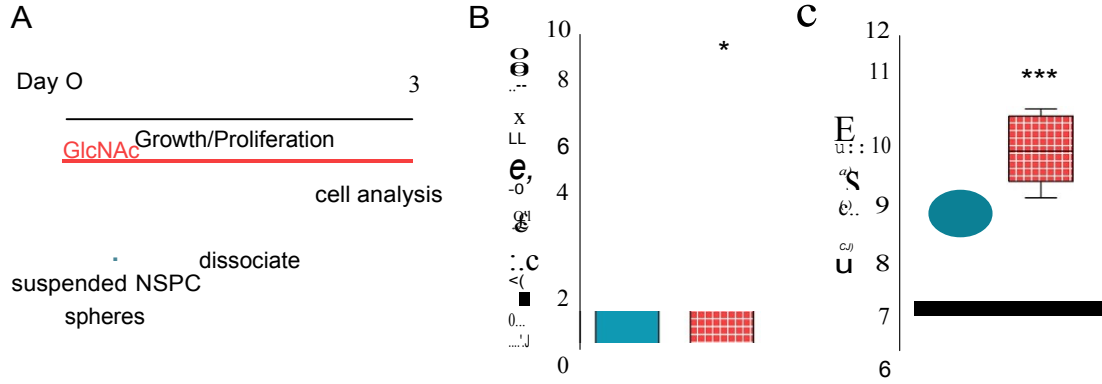
A
Day O
3
GlcNAc
Growth/Proliferation
cell analysis
dissociate
suspended NSPC
spheres
B
10
8
6
4
2
0
*
C
12
11
10
9
8
7
6
***

Untr GlcNAc Untr GlcNAc

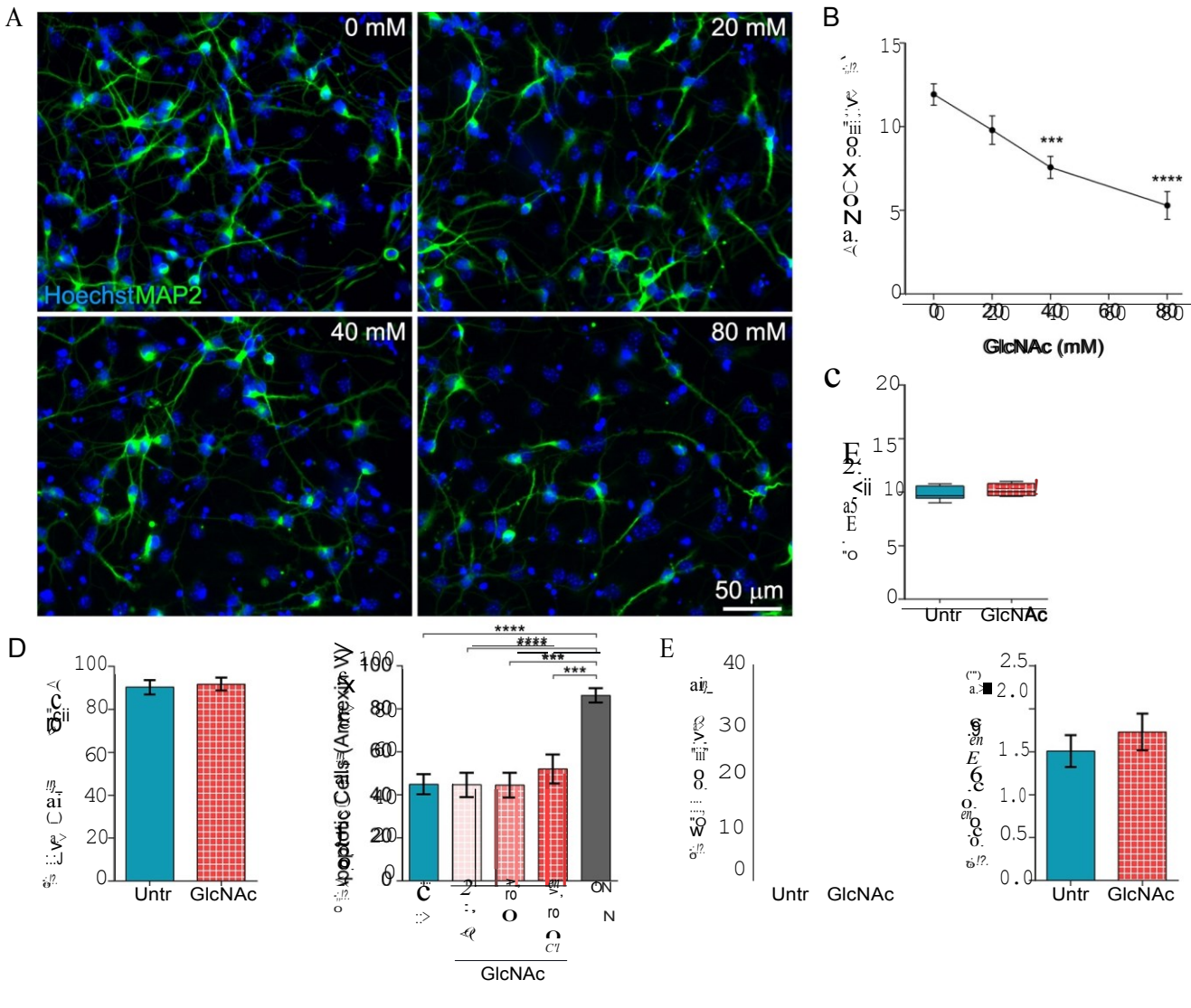
A
0 mM
20 mM
40 mM
80 mM
Hoechst MAP2
50 µm
B
GlcNAc (mM)
***
****
C
Untr
GlcNAc
D
Untr
GlcNAc
****
****
***
***
GlcNAc
E
Untr
GlcNAc
Untr
GlcNAc

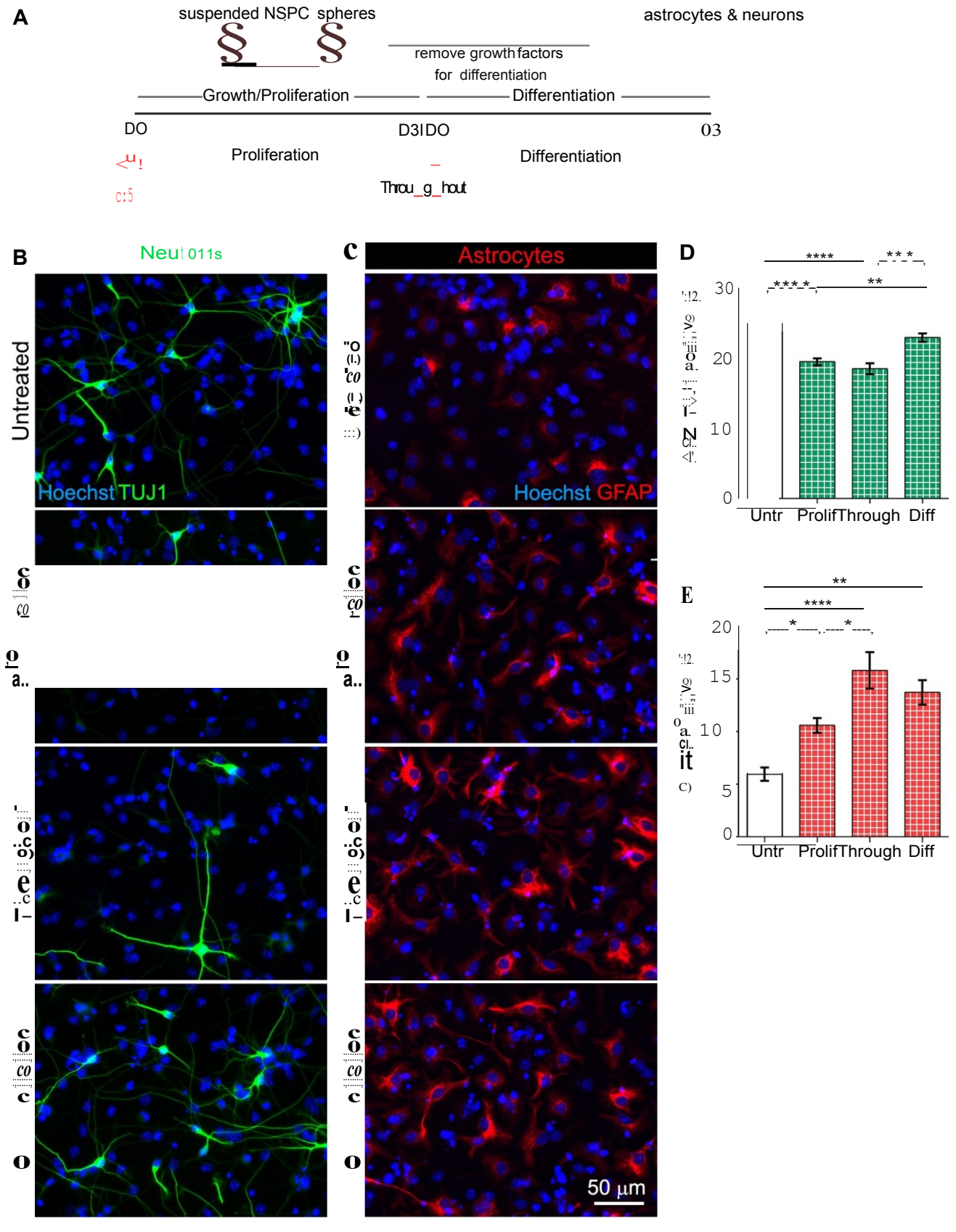
A
suspended NSPC spheres
astrocytes & neurons
remove growth factors
for differentiation
Growth/Proliferation
Differentiation
DO
D3IDO
03
Proliferation
Differentiation
Throu_g_hout
B
Neu! 011s
Untreated
Hoechst TUJ1
C
Astrocytes
Hoechst GFAP
50 µm
D
****
***
**
30
20
10
0
Untr
ProlifThrough
Diff
E
**
****
20
15
10
5
0
Untr
ProlifThrough
Diff

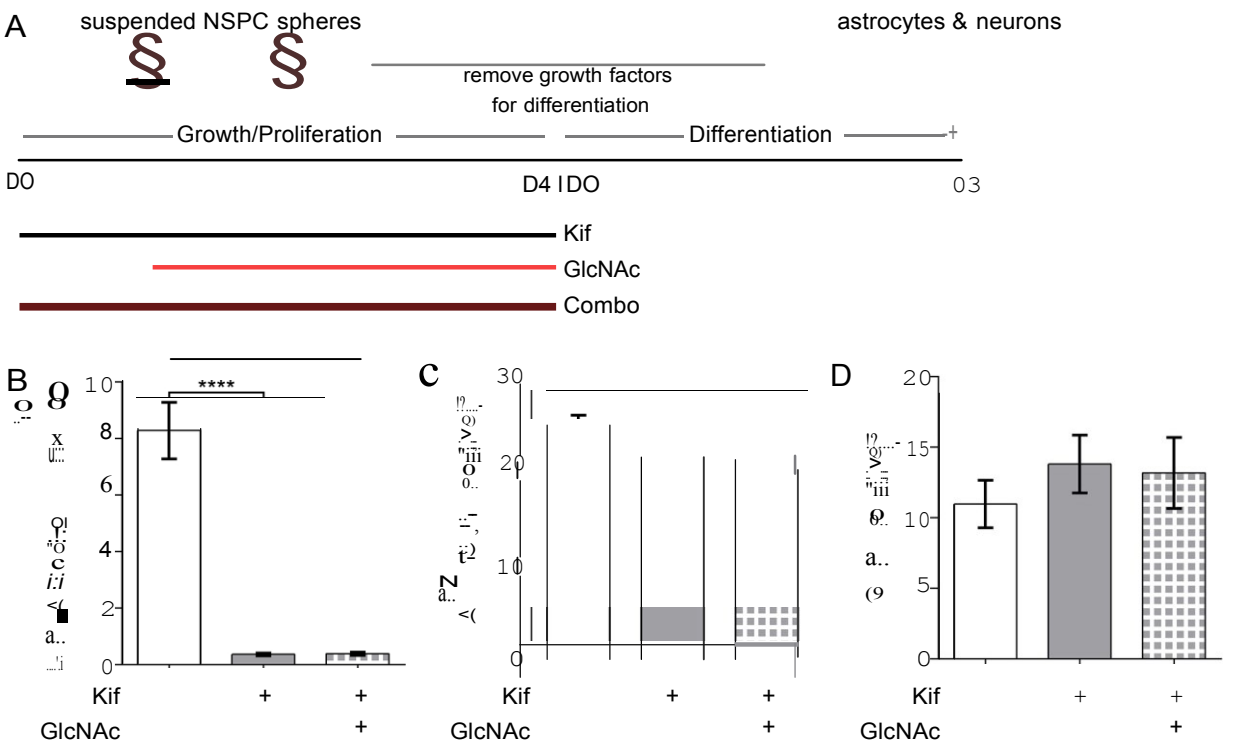
A
suspended NSPC spheres
astrocytes & neurons
remove growth factors
for differentiation
Growth/Proliferation
Differentiation
DO
D4 IDO
03
Kif
GlcNAc
Combo
B
****
Kif
GlcNAc
C
Kif
GlcNAc
D
Kif
GlcNAc